

Aluminum Solubility in Complex Electrolytes - 13011

S. F. Agnew* and C. T. Johnston**

*Columbia Energy and Environmental Services, Inc., 1806 Terminal Dr., Richland, WA 99354

**Dept. of Crop, Soil, and Environmental Sciences, Purdue University, West Lafayette, IN 47907

ABSTRACT

Predicting aluminum solubility for Hanford and Savannah River waste liquids is very important for their disposition. It is a key mission goal at each Site to leach as much aluminum as practical from sludges in order to minimize the amount of vitrified high level waste. And it is correspondingly important to assure that any soluble aluminum does not precipitate during subsequent decontamination of the liquid leachates with ion exchange.

This report shows a very simple and yet thermodynamic model for aluminum solubility that is consistent with a wide range of Al liquors, from simple mixtures of hydroxide and aluminate to over 300 Hanford concentrates and to a set of 19 Bayer liquors for temperatures from 20-100 °C. This dimer- dS_{mix} (DDS) model incorporates an ideal entropy of mixing along with previous reports for the Al dimer, water activities, gibbsite, and bayerite thermodynamics.

We expect this model will have broad application for nuclear wastes as well as the Bayer gibbsite process industry.

INTRODUCTION

Previous reports have shown that aluminum is much more soluble in Hanford tank waste liquids than predicted by simple models [1, 2]. Even sophisticated electrolyte solubility calculations such as OLI's MSE do not always predict the unusually high Al solubilities in many tank concentrates [3]. Figure 1 shows over 300 selected tank waste liquid assays for aluminum versus free hydroxide concentrations [4]. This shows waste assays were selected with a sodium range of 3 to 7 M, which is consistent with sodium processing range for Hanford's planned waste treatment and immobilization plant, WTP.

Previous reports have shown that for Al concentrations in excess of ~1 m, the Al dimer was important [5-7]. At more modest Al concentrations around 0.5 m Al, though, it was carbonate or TOC that correlated with enhanced Al solubility. A later report further showed a correlation between an aluminocarbonate, dawsonite, solubility product and enhanced Al solubility [8].

This paper, though, will show that indeed the Al dimer is important for high aluminate concentrations, even for 0.5 m Al. However, for complex mixtures there is not just a single species like carbonate or TOC that is responsible for enhanced Al solubility in Hanford tank liquids. It is rather the very complexity of these tank liquids as mixtures of many species that is also responsible for enhanced Al solubility in Hanford waste liquids in the sodium 3-7 m Na concentration range.

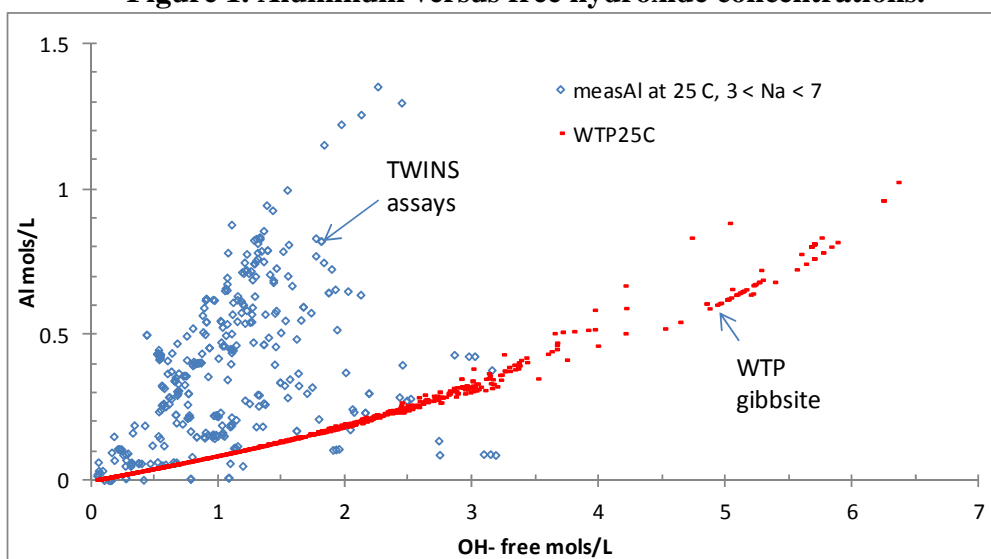
In fact, the ideal entropy of mixing is a well-known [9, 10] and straightforward calculation and ends up being a significant factor even for simple aluminate/NaOH mixtures. This is because,

unlike a simple electrolyte, gibbsite solubility also depends on the presence of a much larger amount of hydroxide.

We show here that the solubility of Al is consistent with a surprisingly simple model that incorporates three key attributes mentioned: the free energy of dissolution for gibbsite or bayerite, the ideal entropy of mixing, and the Al dimer equilibrium.

Equally surprising is this simple model does not directly incorporate activity coefficients. Rather it seems that there is a fortuitous cancellation of activities in the ratio between aluminate and hydroxide. This results in the simple Al solubility equation based on thermodynamics and valid over a wide range of conditions. Furthermore, the ratio of the dimer activity and the square of the monomer activity also does not seem to vary significantly over the range of this study.

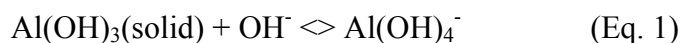
Figure 1. Aluminum versus free hydroxide concentrations.



Measured Al concentration from TWINS (Tank Waste Information Network System) [4] data for total sodium in the range 3 to 7 M. Also shown is the corresponding predictions from the WTP gibbsite solubility at 25 C.

METHODOLOGY

In its simplest form, gibbsite, bayerite, or $\text{Al}(\text{OH})_3$ solubility is



and this expression shows up in much previous work [11]. The corresponding reaction free energy is from Table I and results in an infinite dilution equilibrium as

$$C_{\text{Al}} = K_1 C_{\text{OH}}(\text{m}) \quad (\text{Eq. 2})$$

where

$$K_1 = e^{-\Delta G_r/RT} = e^{-\Delta H_r/RT + \Delta S_r/R + \Delta S_{\text{mix}}/R} \quad (\text{Eq. 3})$$

and ΔG_r , ΔH_r and ΔS_r are the free energy, enthalpy, and entropy of reaction, respectively, and

ΔS_{mix} is the entropy of mixing. Although typical derivations do not explicitly consider the entropy of mixing as in Eq. 3, we show below that this system parameter varies significantly for gibbsite because of the presence of NaOH.

This simple expression as Eq. 1 does not explain either the quadratic dependence of the observed Al solubility in Fig. 1 or the enhanced Al solubility of the tank waste data. In fact, it is quite well known [11-14] that Al solubility is quadratic in increasing hydroxide concentrations as compared to Eq. 1.

Of course, K_1 is typically referred to as an *effective* equilibrium constant or quotient since it does not include electrolyte activity. Activity coefficients are correction factors for each formal concentration whose product results in a thermodynamic activity and the thermodynamic equilibrium constant.

$$\gamma_{\text{Al}} C_{\text{Al}} = \underline{K}_1 \gamma_{\text{OH}} C_{\text{OH}}(m) \quad (\text{Eq. 4})$$

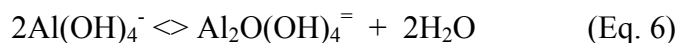
Thus the effective versus thermodynamic equilibrium constants, K_1 versus \underline{K}_1 are proportional to the ratio of activity coefficients for hydroxide and Al.

$$K_1 = \underline{K}_1 \gamma_{\text{OH}} / \gamma_{\text{Al}} \quad (\text{Eq. 5})$$

In what follows, we will assume that the hydroxide and aluminate activity coefficients are equal and therefore that the ratio is ~ 1 .

Aluminate Dimer Equilibrium

In addition to the aluminate monomer, the aluminate dimer has been reported [5-7] as



$$K_2 = \{(1-f) / (2 f^2)\} a_w^2 / C_{\text{Al}} \quad (\text{Eq. 7})$$

where K_2 is the reported effective equilibrium constant and the concentration of Al as monomer, $C_{\text{Al}2}$, is then

$$C_{\text{Al}2} = C_{\text{Al}} \frac{\sqrt{1 + 8C_{\text{Al}} K_2 / a_w^2} - 1}{4K_2 / a_w^2} \quad (\text{Eq. 8})$$

Two waters of hydration appear in this expression to better represent the equilibrium data compared with just one water. Once again, this *effective* K_2 is proportional to the thermodynamic \underline{K}_2 by the ratio of dimer and the square of monomer activity constant as

$$K_2 = \underline{K}_2 \gamma_{\text{dimer}} / \gamma_{\text{Al}}^2 \quad (9)$$

Over the range of aluminate dimer of this study, we will assume that this activity ratio is constant.

Entropy of Mixing

The entropy of mixing is well-known [9, 10] and the expression for an ideal mixture is in terms of mol fraction or total molality, m , as

$$\Delta S_{mix} = -R \sum x_i \ln x_i = R \left(\frac{\ln(1 + m/55.51)}{1 + m/55.51} + \sum_i \frac{\ln(55.51/f_i m + \sum_j f_j/f_i)}{55.51/f_i m + \sum_j f_j/f_i} \right) \quad (\text{Eq. 10})$$

$$f_j = \frac{v_j m_j}{\sum_i v_i m_i} \quad \sum_j f_j = 1 \quad (\text{Eq. 11})$$

$$f_{Na} = m \sum_i f_i \frac{z_i^+}{(z_i^+ + z_i^-)} \approx \frac{1}{2} \quad f_{iX} = \frac{z_i^-}{(z_i^+ + z_i^-)} \quad (\text{Eq. 12})$$

$$\gamma_{mix} = (1 + m/55.51)^{1/(1+m/55.51)} \prod_i \left(\frac{55.51}{f_i m} + \frac{1}{f_i} \right)^{f_i m / (m + 55.51)} \quad (\text{Eq. 13})$$

$$\gamma_{mix} = \left(1 + \frac{m}{55.51} \right)^{1/(1+m/55.51)} \left(\frac{1}{f_{iNa}} + \frac{55.51}{f_{iNa} m} \right)^{f_{iNa} m / (m + 55.51)} \prod_i \left(\frac{55.51}{f_i f_{iX} m} + \frac{1}{f_i f_{iX}} \right)^{f_i f_{iX} m / (m + 55.51)} \quad (\text{Eq. 14})$$

SCE Water Activity

The equilibrium calculation for the aluminum dimer depends on water activity. To estimate water activity, we used the solvation cluster equilibria (SCE) model for the mixtures [2].

$$a_w = \frac{1}{1 + \frac{\sum v_i m_i}{55.51} + \gamma_{mix} \left(\frac{1}{1 + \frac{\sum v_i m_i}{55.51}} \right)^n \prod (K_i \gamma_{iDH})^{f_i n_i}} \quad (\text{Eq. 15})$$

K_i = SCE hydration equilibrium constant

n_i = SCE hydration order, m_i is molality of electrolyte i

v_i = the SCE effective ion number for electrolyte i

f_i = fraction of electrolyte i

γ_{iDH} = Debye-Hückel factor, Eq. 16 (no parameters)

$A_\gamma = 1.1723$, Debye-Hückel constant

γ_{mix} = entropy of mixing factor, Eq. 14 (no parameters)

$n = \sum f_i n_i$, weighted average n

z_{i+} , z_{i-} , cation and anion charge numbers for electrolyte i

I = ionic strength, $\frac{1}{2} \sum m_i z_i^2$

$$\ln \gamma_{iDH} = \frac{A_\gamma}{\frac{1}{I^{1/2}} + 1} \sum f_i \frac{n_i}{n} z_{i+} z_{i-} \quad (\text{Eq. 16})$$

For the well defined mixtures, we have used SCE parameters model and parameters reported [2] for each of the pure electrolytes. For the Hanford tank waste liquids, however, we have used K_i and n_i for NaOH to represent NaOH and NaAl(OH)₄ and for NaNO₂ to represent all other electrolytes to estimate water activity of assayed liquids. This was necessary since there was

limited information on many of the electrolytes like total organic carbon, TOC for example, which is important but represents a large number of species.

Table I. Thermodynamic Parameters for Gibbsite and Bayerite.

	K_1	dG_R J/mol	dH_R J/mol	dS_R J/mol/deg	K_2	T °C
gibbsite* Russell/WTP	0.063	6,850	22,000	50.9	0.093	40-100
bayerite EQ3/6 TWINS/Barney fit	0.16	4,500	17,100	42.0	0.093	25
gibbsite* EQ3/6	0.075	6,410	22,300	53.3		25

**The gibbsite thermodynamics from EQ3/6 is a compendium of values extrapolated to infinite dilution without explicit inclusion of the entropy of mixing. Thus the Russell gibbsite fit with separate ΔS_{mix} differs slightly from EQ3/6.*

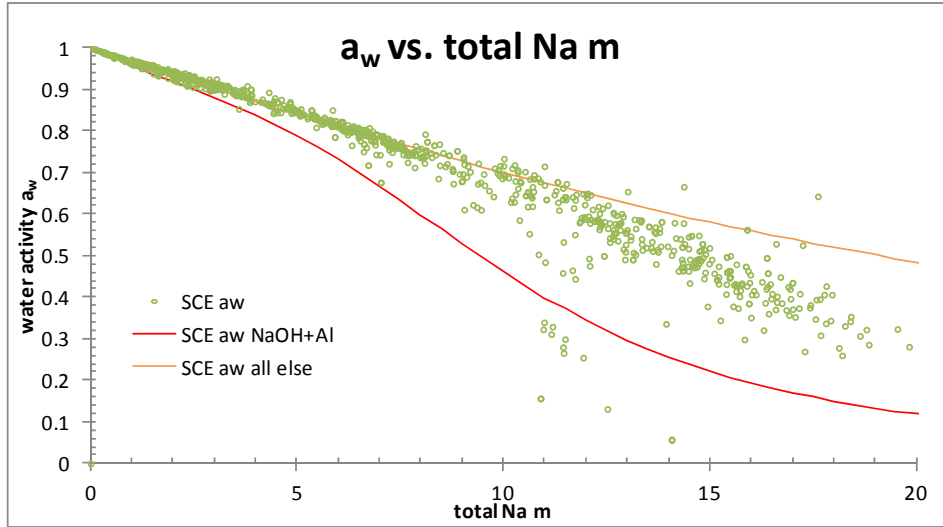
***These parameters do yet have uncertainties and the three significant figures shown are merely nominal.*

Table II. Parameters for SCE water activity.

	K_i	n_i	v_i
NaOH and NaAl(OH) ₄	7.53	6.14	2.0
NaNO ₂ and all else	4.81	4.16	2.0

The advantage of the SCE approach for water activity is that it provides a great deal of flexibility for estimating water activity for such complex mixtures as Hanford tank wastes.

Figure 2. Water activity versus total sodium concentration, Na m.



Plot of calculated SCE water activities (Eq. 15) for 966 TWINS assays versus sodium molality along with water activity for sodium hydroxide/aluminate and sodium nitrite and all else as described in text.

DDS Aluminate Solubility

The dimer- dS_{mix} (DDS) solubility calculation follows from above as

$$C_{Al} = C_{OH} e^{-\Delta G_R / RT + \Delta S_{mix} / R} + 2C_{Al2} \quad (\text{Eq. 17})$$

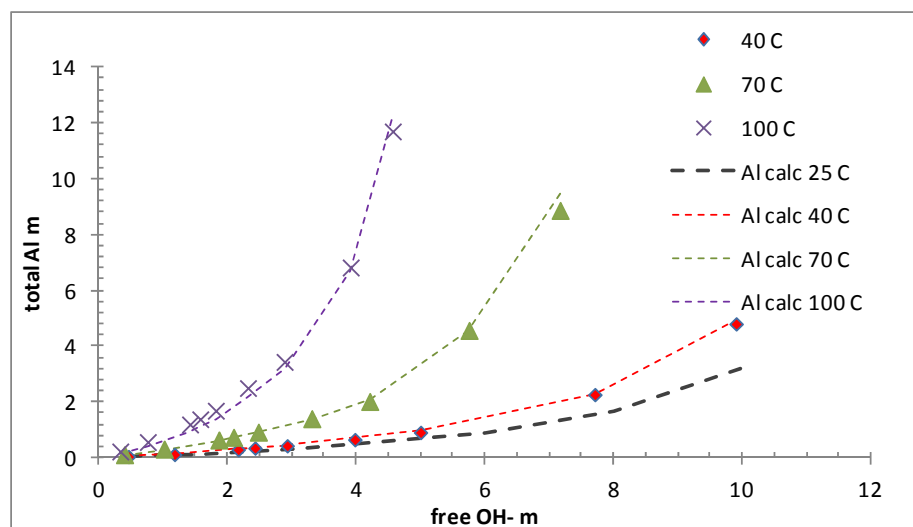
$$C_{Al} = C_{OH} e^{-\Delta G_R / RT + \Delta S_{mix} / R} \left(2 - \frac{\sqrt{1 + 8C_{Al} K_2 / a_w^2} - 1}{2K_2 / a_w^2} \right) \quad (\text{Eq. 18})$$

where the aluminate solubility, C_{Al} , is still proportional to hydroxide concentration, C_{OH} , but the dimer factor has further dependences on the dimer equilibrium constant and water activity.

RESULTS AND DISCUSSION

The dimer enthalpy and entropy of reaction of Eq. 18 was adjusted to fit the gibbsite solubility data [14] versus temperature as shown in Fig. 3. In addition, Fig. 3 shows the extrapolated data for 25 C, which was not reported in this paper. Since the DDS methodology explicitly calculates the entropy of mixing as explained above, the thermodynamic constants for gibbsite different somewhat from those of other sources.

Figure 3. Gibbsite solubility versus free hydroxide.



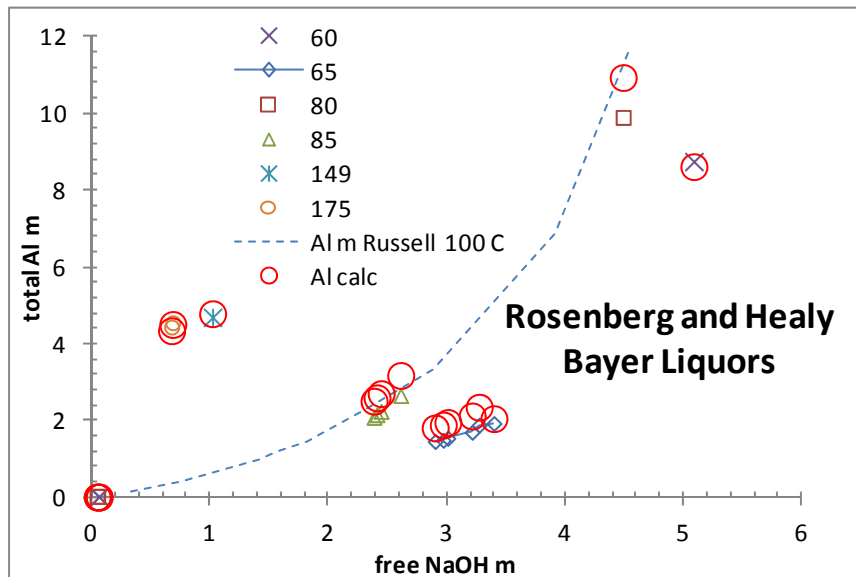
Gibbsite solubility data [14] along with fit of Eq. 18 to derive gibbsite and dimer data shown in Table I.

The fit of Eq. 18 to the gibbsite solubilities in Fig. 3 result in the dimer parameters of Table I, and then using Table I parameters, Fig. 4 compares Eq. 18 DDS predictions for gibbsite solubility for a dataset for Bayer liquor aluminate solubilities [15] as a function of hydroxide. The DDS aluminate solubility predictions of Eq. 18 appear to represent the Bayer liquor dataset gibbsite solubilities very well.

We then compared total Al solubility predictions by DDS the a of Hanford tank liquid assays for aluminate. The TWINS Al assays [4] in Figs. 5 and 6 show limiting aluminate solubilities that are consistent with the same DDS aluminate solubility, Eq. 18, given the parameters in Table I for bayerite. Since it is not all of the Hanford tank liquid assays are saturated in aluminate, Fig. 6 shows that the DDS aluminate solubility is consistent with a limiting solubility of a large number of the 966 aluminate assays from tank liquids. Table III shows the average composition of Hanford tank liquids upon dilution to 5.0 M Na.

For Hanford solutions, bayerite and not gibbsite seems to limit the solubility and Fig. 5 shows those two limits plotted. Bayerite is roughly twice as soluble as gibbsite and bayerite has been observed to limit aluminum in the presence of carbonate [18, 19].

Figure 4. Calculated versus measured total Bayer Al versus free hydroxide.



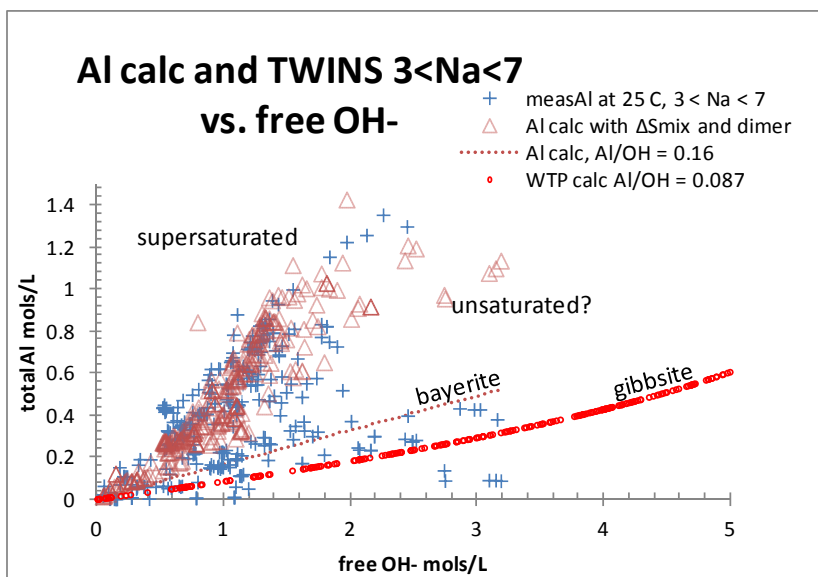
Plot of measured Al solubility (various markers) as function of free OH^- for a range of temperatures (65-175 C) and concentrations from Rosenberg and Healy 1996 [15]. Predictions from Eq. 18 (red circles) use gibbsite parameters from Table I.

Having such a simple expression for aluminate solubility as Eq. 18 that is consistent with limiting solubilities for such a large variation of solutions and temperatures suggests an underlying simplicity for aluminate solubility. That is, the activity factors for aluminate and hydroxide seem to be nearly equal and their ratio is therefore close to unity.

The dehydration dimer of aluminate has been observed in Raman spectra and reported many times in the past. Although various equilibrium constants have been reported, the relative intensities of Raman features associated with dimer versus monomer have never been established. The fit of the data in Fig. 3 represents the first report of the dimer equilibrium that accounts for the dimer versus monomer amounts consistent with the measured gibbsite solubilities in Fig. 3.

Table III provides average Hanford tank waste liquid and slurry compositions showing the major electrolytes and solids present. There are in addition a large number of minor components as well.

Figure 5. Calculated and measured total Hanford tank Al versus free hydroxide.



These selected liquid assays ranged in total Na from 3 to 7 M and show Al in mols/L as reported by TWINS (+). Also shown are the calculations by Eq. 18 (Δ) with bayerite parameters in Table 1 along with the WTP gibbsite (o) and bayerite (...) calculations, all at 25 C.

Table III. Average Hanford tank waste liquid and solid compositions given dilution to 5.0 M Na.

Average liquid feed composition after retrieval		Average sludge feed composition after retrieval	
Soln.	M mols/L	Slurry	10-15 wt%
Na ⁺	5.0	Al(OH) ₃	6.1 wt%
NO ₃ ⁻	1.6	FeOOH	0.7 wt%
NO ₂ ⁻	0.63	Na ₃ PO ₄	0.6 wt%
OH ⁻	0.58	Na ₂ CO ₃	0.4 wt%
Al(OH) ₄ ⁻	0.28	CrOOH	0.2 wt%
CO ₃ ⁼	0.31	...	
PO ₄ ³⁻	0.09		
SO ₄ ⁼	0.08		
TOC	0.09		
...			

Figure 6. Calculated versus measured total Al.

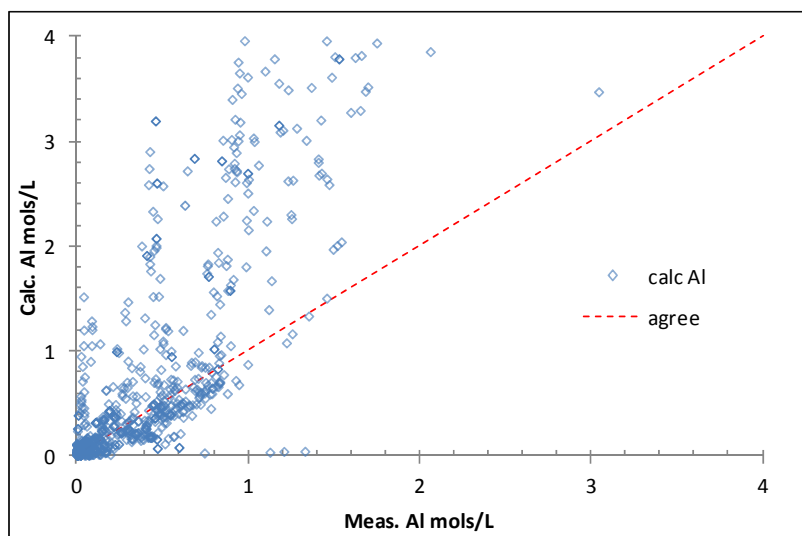


Figure 6. Plot of measured versus calculated aluminum molarity by the DDS for 966 assays of Hanford tank liquids from TWINS ranging from dilute to 12 M Na.

SUMMARY

The dimer/ dS_{mix} (DDS) model is a relatively simple thermodynamic model that is consistent with reported aluminum solubility over very wide ranges of compositions and temperatures. If it were to be further validated, the DDS model could prove quite useful for a wide range of applications.

It is not often that work with nuclear waste concentrates provides insight into industrial chemistry. Not only is it apparent that the aluminate dimer and therefore water activity have important roles in aluminate solubility, the very complexity of each mixture must be very carefully accounted for in any thermodynamic parameterization. In particular, fitting parameterized activity functions to Al solubility data will not scale correctly without proper consideration of dimer, water activity, and entropy of mixing for these complex mixtures.

The quality assurance that was applied for this paper is consistent with current policy for the application intended.

ACKNOWLEDGEMENTS

Thanks to Department of Energy EM, Washington River Protection Solutions, and Columbia Energy and Environmental for support of this project.

REFERENCES

1. Agnew, S.F., J.G. Reynolds, C.T. Johnston, "Aluminum Solubility Model for Hanford Tank Waste Treatment," Proceedings of Waste Management Conference, Mar. 1-5, Phoenix, AZ, 2009.
2. Agnew, S.F., J.G. Reynolds, C.T. Johnston, "Predicting Water Acitivity for Complex Wastes with Solvation Cluster Equilibria (SCE)," Proceedings of Waste Management Conference, Feb. 26 - Mar. 1, 2012, Phoenix, AZ.
3. Wang, P, A. Anderko, R.D. Young, R.D. Springer, A Comprehensive Model for Calculating Phase Equilibria and Thermophysical Properties of Electrolytic Systems, OLI Systems, Inc., 2008.
4. Bobrowski, S. F., and D. Lee, *Tank Waste Information Network System (TWINS)*, PNNL-SA-45730, December 2008.
5. Johnston, C. T.; Agnew, S. F.; Schoonover, J. R.; Kenney, III, J. W.; Page, B.; Osborn, J.; Corbin, R., *Raman Study of Aluminum Speciation in Simulated Alkaline Nuclear Waste*, Environ. Sci. Technol., 36 (11), 2451-8, 2002.
6. Sipos, P., Capewell, S.G., May, P.M., Hefter, G.T., Laurency, G., Lukacs, F., and Roulet, R. (1998) *Spectroscopic studies of the chemical speciation in concentrated alkaline aluminate solutions*. *J.Chem.Soc.Dalton Trans.* 3007-3012.
7. Moolenaar, R J., J. C. Evans, and L. D. McKeever, *The Structure of the Aluminate Ion in Solution at High pH*, J. Phys. Chem., 74, 3629,1970.
8. Agnew, S.F., *Role of Dawsonite in Aluminum Solubility for Hanford Tank Waste Treatment*, in Proceedings of Waste Management Conference, Mar. 7-11, Phoenix, AZ, 2010.
9. Glasstone, S., *Textbook of Physical Chemistry*, MacMillan and Co. Ltd., London, 1966.
10. Lewis, G.N., M. Randall, K.S. Pitzer, L. Brewer, *Thermodynamics*, McGraw-Hill, New York, NY, 1961.
11. Apps, J. A., J. M. Neil, and C.-H. Jun, *Thermochemical Properties of Gibbsite, Bayerite, Boehmite, Diaspore, and the Aluminate Ion Between 0 and 350°C*, NUREG/CR--5271, Lawrence Berkeley Laboratory, Berkeley, CA, 1989.
12. Reynolds, J.G. *Gibbsite Solubility Model*, Contract No. DE-AC27-01RV14136 -CCN 160514, SUPERCEDES CCN 137192, July 2007.
13. Reynolds, D. A., *Practical Modeling of Aluminum Species in High-pH Waste*, WHC-EP-0872, Westinghouse Hanford Company, Richland, Washington, 1995.
14. Russell, A.S.; Edwards, J.D.; Taylor, C.S., *Solubility and Density of Hydrated Aluminas in NaOH Solutions*, J. Metals, 1123, Trans. American Inst. Metallurgical Eng., 1955.
15. Rosenberg, S.P., S.J. Healy, A Thermodynamic Model for Gibbsite Solubility in Bayer Liquors, in Fourth International Alumina Quality Workshop, Darwin, AUS, 301-310, 1996.
16. Zhou, J., Q.Y. Chen, J. Li, Z.L.Yin, X.Zhou, P.M. Zhang, "Isopiestic measurement for the osmotic and activity coefficients for the NaOH-NaAl(OH)₄-H₂O sytem at 313.2 K," *Geochim.Cosmochem.Acta*, 67, 3459-72, 2003.
17. Szabo, Z.G., J. Wajano, K. Burger, "Investigation of the complex equilibria by water-activity measurement," *Acta Chem. Acad. Sci. Hun.*, 86, 147-58, 1975.
18. Zhang, G.Y., Y.F. Hu, R.K. Xu, J. Dynes, R.I.R. Blyth, L.M. Kozak, P.M. Huang, *Carbonate-Induced Structural Perturbation of Al Hydroxides*, *Clays and Clay Minerals*, 57, 795-807, 2009.

19. P. Benezeth, D. A. Palmer, L.M. Anovitz, J. Horita, *Dawsonite Synthesis and Reevaluation of Its Thermodynamic Properties from Solubility Measurements: Implications for Mineral Trapping of CO₂*, *Geochimica et Cosmica Acta* 71, 4438-55, 2007.